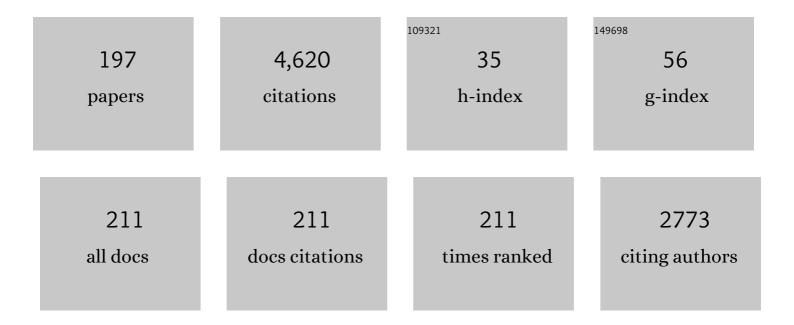
Anita Layton

List of Publications by Year in descending order

Source: https://exaly.com/author-pdf/3235062/publications.pdf Version: 2024-02-01



#	Article	IF	CITATIONS
1	Numerical Methods for Fluid-Structure Interaction — A Review. Communications in Computational Physics, 2012, 12, 337-377.	1.7	472
2	Predicted consequences of diabetes and SGLT inhibition on transport and oxygen consumption along a rat nephron. American Journal of Physiology - Renal Physiology, 2016, 310, F1269-F1283.	2.7	118
3	High-order multi-implicit spectral deferred correction methods for problems of reactive flow. Journal of Computational Physics, 2003, 189, 651-675.	3.8	111
4	Modeling Vesicle Traffic Reveals Unexpected Consequences for Cdc42p-Mediated Polarity Establishment. Current Biology, 2011, 21, 184-194.	3.9	111
5	Modeling oxygen consumption in the proximal tubule: effects of NHE and SGLT2 inhibition. American Journal of Physiology - Renal Physiology, 2015, 308, F1343-F1357.	2.7	110
6	SGLT2 inhibition in a kidney with reduced nephron number: modeling and analysis of solute transport and metabolism. American Journal of Physiology - Renal Physiology, 2018, 314, F969-F984.	2.7	100
7	On the accuracy of finite difference methods for elliptic problems with interfaces. Communications in Applied Mathematics and Computational Science, 2006, 1, 91-119.	1.8	83
8	A region-based mathematical model of the urine concentrating mechanism in the rat outer medulla. I. Formulation and base-case results. American Journal of Physiology - Renal Physiology, 2005, 289, F1346-F1366.	2.7	79
9	Urine-Concentrating Mechanism in the Inner Medulla. Clinical Journal of the American Society of Nephrology: CJASN, 2014, 9, 1781-1789.	4.5	75
10	A computational model for simulating solute transport and oxygen consumption along the nephrons. American Journal of Physiology - Renal Physiology, 2016, 311, F1378-F1390.	2.7	74
11	Two modes for concentrating urine in rat inner medulla. American Journal of Physiology - Renal Physiology, 2004, 287, F816-F839.	2.7	72
12	Solute transport and oxygen consumption along the nephrons: effects of Na ⁺ transport inhibitors. American Journal of Physiology - Renal Physiology, 2016, 311, F1217-F1229.	2.7	72
13	Implications of the Choice of Quadrature Nodes for Picard Integral Deferred Corrections Methods for Ordinary Differential Equations. BIT Numerical Mathematics, 2005, 45, 341-373.	2.0	70
14	Conservative multi-implicit spectral deferred correction methods for reacting gas dynamics. Journal of Computational Physics, 2004, 194, 697-715.	3.8	68
15	Functional implications of sexual dimorphism of transporter patterns along the rat proximal tubule: modeling and analysis. American Journal of Physiology - Renal Physiology, 2018, 315, F692-F700.	2.7	68
16	Role of three-dimensional architecture in the urine concentrating mechanism of the rat renal inner medulla. American Journal of Physiology - Renal Physiology, 2008, 295, F1271-F1285.	2.7	67
17	A numerically efficient and stable algorithm for animating water waves. Visual Computer, 2002, 18, 41-53.	3.5	62
18	Impact of renal medullary three-dimensional architecture on oxygen transport. American Journal of Physiology - Renal Physiology, 2014, 307, F263-F272.	2.7	61

#	Article	IF	CITATIONS
19	Functional implications of the sex differences in transporter abundance along the rat nephron: modeling and analysis. American Journal of Physiology - Renal Physiology, 2019, 317, F1462-F1474.	2.7	56
20	Sex differences in solute transport along the nephrons: effects of Na ⁺ transport inhibition. American Journal of Physiology - Renal Physiology, 2020, 319, F487-F505.	2.7	56
21	A mathematical model of O ₂ transport in the rat outer medulla. I. Model formulation and baseline results. American Journal of Physiology - Renal Physiology, 2009, 297, F517-F536.	2.7	55
22	A mathematical model of the urine concentrating mechanism in the rat renal medulla. I. Formulation and base-case results. American Journal of Physiology - Renal Physiology, 2011, 300, F356-F371.	2.7	51
23	Adaptive changes in GFR, tubular morphology, and transport in subtotal nephrectomized kidneys: modeling and analysis. American Journal of Physiology - Renal Physiology, 2017, 313, F199-F209.	2.7	48
24	Modeling within-Host SARS-CoV-2 Infection Dynamics and Potential Treatments. Viruses, 2021, 13, 1141.	3.3	48
25	Sex-specific long-term blood pressure regulation: Modeling and analysis. Computers in Biology and Medicine, 2019, 104, 139-148.	7.0	46
26	A mathematical model of the myogenic response to systolic pressure in the afferent arteriole. American Journal of Physiology - Renal Physiology, 2011, 300, F669-F681.	2.7	45
27	The Mammalian Urine Concentrating Mechanism: Hypotheses and Uncertainties. Physiology, 2009, 24, 250-256.	3.1	44
28	Effects of pH and medullary blood flow on oxygen transport and sodium reabsorption in the rat outer medulla. American Journal of Physiology - Renal Physiology, 2010, 298, F1369-F1383.	2.7	44
29	Role of thin descending limb urea transport in renal urea handling and the urine concentrating mechanism. American Journal of Physiology - Renal Physiology, 2011, 301, F1251-F1259.	2.7	44
30	Autoregulation and conduction of vasomotor responses in a mathematical model of the rat afferent arteriole. American Journal of Physiology - Renal Physiology, 2012, 303, F229-F239.	2.7	44
31	A region-based mathematical model of the urine concentrating mechanism in the rat outer medulla. II. Parameter sensitivity and tubular inhomogeneity. American Journal of Physiology - Renal Physiology, 2005, 289, F1367-F1381.	2.7	43
32	Functional implications of the three-dimensional architecture of the rat renal inner medulla. American Journal of Physiology - Renal Physiology, 2010, 298, F973-F987.	2.7	43
33	Urine concentrating mechanism: impact of vascular and tubular architecture and a proposed descending limb urea-Na ⁺ cotransporter. American Journal of Physiology - Renal Physiology, 2012, 302, F591-F605.	2.7	43
34	A mathematical model of O ₂ transport in the rat outer medulla. II. Impact of outer medullary architecture. American Journal of Physiology - Renal Physiology, 2009, 297, F537-F548.	2.7	42
35	Effects of NKCC2 isoform regulation on NaCl transport in thick ascending limb and macula densa: a modeling study. American Journal of Physiology - Renal Physiology, 2014, 307, F137-F146.	2.7	42
36	A mathematical model of the urine concentrating mechanism in the rat renal medulla. II. Functional implications of three-dimensional architecture. American Journal of Physiology - Renal Physiology, 2011, 300, F372-F384.	2.7	41

#	Article	IF	CITATIONS
37	A computational model of epithelial solute and water transport along a human nephron. PLoS Computational Biology, 2019, 15, e1006108.	3.2	41
38	Interactions among mTORC, AMPK and SIRT: a computational modelÂfor cell energyÂbalance and metabolism. Cell Communication and Signaling, 2021, 19, 57.	6.5	41
39	Multistability in tubuloglomerular feedback and spectral complexity in spontaneously hypertensive rats. American Journal of Physiology - Renal Physiology, 2006, 291, F79-F97.	2.7	40
40	Theoretical assessment of renal autoregulatory mechanisms. American Journal of Physiology - Renal Physiology, 2014, 306, F1357-F1371.	2.7	40
41	Renal hemodynamics, function, and oxygenation during cardiac surgery performed on cardiopulmonary bypass: a modeling study. Physiological Reports, 2015, 3, e12260.	1.7	40
42	A region-based model framework for the rat urine concentrating mechanism. Bulletin of Mathematical Biology, 2003, 65, 859-901.	1.9	39
43	Sex differences in solute and water handling in the human kidney: Modeling and functional implications. IScience, 2021, 24, 102667.	4.1	35
44	Multistable Dynamics Mediated by Tubuloglomerular Feedback in a Model of Coupled Nephrons. Bulletin of Mathematical Biology, 2009, 71, 515-555.	1.9	34
45	Urine concentrating mechanism in the inner medulla of the mammalian kidney: role of threeâ€dimensional architecture. Acta Physiologica, 2011, 202, 361-378.	3.8	34
46	Targeted delivery of solutes and oxygen in the renal medulla: role of microvessel architecture. American Journal of Physiology - Renal Physiology, 2014, 307, F649-F655.	2.7	34
47	Impacts of nitric oxide and superoxide on renal medullary oxygen transport and urine concentration. American Journal of Physiology - Renal Physiology, 2015, 308, F967-F980.	2.7	34
48	Renal potassium handling in rats with subtotal nephrectomy: modeling and analysis. American Journal of Physiology - Renal Physiology, 2018, 314, F643-F657.	2.7	34
49	How Do Kidneys Adapt to a Deficit or Loss in Nephron Number?. Physiology, 2019, 34, 189-197.	3.1	34
50	Feedback-mediated dynamics in a model of a compliant thick ascending limb. Mathematical Biosciences, 2010, 228, 185-194.	1.9	33
51	Bladder urine oxygen tension for assessing renal medullary oxygenation in rabbits: experimental and modeling studies. American Journal of Physiology - Regulatory Integrative and Comparative Physiology, 2016, 311, R532-R544.	1.8	33
52	Sex-specific computational models of the spontaneously hypertensive rat kidneys: factors affecting nitric oxide bioavailability. American Journal of Physiology - Renal Physiology, 2017, 313, F174-F183.	2.7	33
53	The mixed blessing of AMPK signaling in Cancer treatments. BMC Cancer, 2022, 22, 105.	2.6	32
54	Modeling sex differences in the renin angiotensin system and the efficacy of antihypertensive therapies. Computers and Chemical Engineering, 2018, 112, 253-264.	3.8	31

#	Article	IF	CITATIONS
55	Renal medullary and urinary oxygen tension during cardiopulmonary bypass in the rat. Mathematical Medicine and Biology, 2017, 34, dqw010.	1.2	30
56	Impact of nitric-oxide-mediated vasodilation and oxidative stress on renal medullary oxygenation: a modeling study. American Journal of Physiology - Renal Physiology, 2016, 310, F237-F247.	2.7	30
57	Modeling Water Transport across Elastic Boundaries Using an Explicit Jump Method. SIAM Journal of Scientific Computing, 2006, 28, 2189-2207.	2.8	29
58	Predicted effect of circadian clock modulation of NHE3 of a proximal tubule cell on sodium transport. American Journal of Physiology - Renal Physiology, 2018, 315, F665-F676.	2.7	28
59	Recent advances in sex differences in kidney function. American Journal of Physiology - Renal Physiology, 2019, 316, F328-F331.	2.7	28
60	Using integral equations and the immersed interface method to solve immersed boundary problems with stiff forces. Computers and Fluids, 2009, 38, 266-272.	2.5	27
61	Implications of the choice of predictors for semi-implicit Picard integral deferred correction methods. Communications in Applied Mathematics and Computational Science, 2007, 2, 1-34.	1.8	27
62	Understanding sex differences in long-term blood pressure regulation: insights from experimental studies and computational modeling. American Journal of Physiology - Heart and Circulatory Physiology, 2019, 316, H1113-H1123.	3.2	26
63	Mathematical modeling of renal hemodynamics in physiology and pathophysiology. Mathematical Biosciences, 2015, 264, 8-20.	1.9	24
64	Network centrality analysis of eye-gaze data in autism spectrum disorder. Computers in Biology and Medicine, 2019, 111, 103332.	7.0	24
65	Adaptive changes in single-nephron GFR, tubular morphology, and transport in a pregnant rat nephron: modeling and analysis. American Journal of Physiology - Renal Physiology, 2022, 322, F121-F137.	2.7	24
66	On the choice of correctors for semi-implicit Picard deferred correction methods. Applied Numerical Mathematics, 2008, 58, 845-858.	2.1	23
67	Electrohydrodynamics of a viscous drop with inertia. Physical Review E, 2016, 93, 053114.	2.1	23
68	Generation and phenotypic analysis of mice lacking all urea transporters. Kidney International, 2017, 91, 338-351.	5.2	23
69	A Computational Model of Kidney Function in a Patient with Diabetes. International Journal of Molecular Sciences, 2021, 22, 5819.	4.1	23
70	Calcium dynamics underlying the myogenic response of the renal afferent arteriole. American Journal of Physiology - Renal Physiology, 2014, 306, F34-F48.	2.7	22
71	Countercurrent multiplication may not explain the axial osmolality gradient in the outer medulla of the rat kidney. American Journal of Physiology - Renal Physiology, 2011, 301, F1047-F1056.	2.7	21
72	A regularization method for the numerical solution of periodic Stokes flow. Journal of Computational Physics, 2013, 236, 187-202.	3.8	21

#	Article	IF	CITATIONS
73	Dominant factors that govern pressure natriuresis in diuresis and antidiuresis: a mathematical model. American Journal of Physiology - Renal Physiology, 2014, 306, F952-F969.	2.7	21
74	Modeling glucose metabolism and lactate production in the kidney. Mathematical Biosciences, 2017, 289, 116-129.	1.9	21
75	Sex-specific computational models for blood pressure regulation in the rat. American Journal of Physiology - Renal Physiology, 2020, 318, F888-F900.	2.7	21
76	Understanding the dynamics of SARS-CoV-2 variants of concern in Ontario, Canada: a modeling study. Scientific Reports, 2022, 12, 2114.	3.3	21
77	Dynamic contrast-enhanced quantitative susceptibility mapping with ultrashort echo time MRI for evaluating renal function. American Journal of Physiology - Renal Physiology, 2016, 310, F174-F182.	2.7	20
78	Mathematical Modeling in Renal Physiology. Lecture Notes on Mathematical Modelling in the Life Sciences, 2014, , .	0.4	19
79	Control and Modulation of Fluid Flow in the Rat Kidney. Bulletin of Mathematical Biology, 2013, 75, 2551-2574.	1.9	18
80	Transport efficiency and workload distribution in a mathematical model of the thick ascending limb. American Journal of Physiology - Renal Physiology, 2013, 304, F653-F664.	2.7	18
81	Aging affects circadian clock and metabolism and modulates timing of medication. IScience, 2021, 24, 102245.	4.1	18
82	Modeling Glucose Metabolism in the Kidney. Bulletin of Mathematical Biology, 2016, 78, 1318-1336.	1.9	17
83	Modeling Transport and Flow Regulatory Mechanisms of the Kidney. , 2012, 2012, 1-18.		17
84	A semi-Lagrangian double Fourier method for the shallow water equations on the sphere. Journal of Computational Physics, 2003, 189, 180-196.	3.8	16
85	Nitric oxide and superoxide transport in a cross section of the rat outer medulla. I. Effects of low medullary oxygen tension. American Journal of Physiology - Renal Physiology, 2010, 299, F616-F633.	2.7	15
86	Modulation of outer medullary NaCl transport and oxygenation by nitric oxide and superoxide. American Journal of Physiology - Renal Physiology, 2011, 301, F979-F996.	2.7	15
87	Isolated interstitial nodal spaces may facilitate preferential solute and fluid mixing in the rat renal inner medulla. American Journal of Physiology - Renal Physiology, 2012, 302, F830-F839.	2.7	15
88	Effect of tubular inhomogeneities on feedback-mediated dynamics of a model of a thick ascending limb. Mathematical Medicine and Biology, 2013, 30, 191-212.	1.2	15
89	Cubic Spline Collocation Method for the Shallow Water Equations on the Sphere. Journal of Computational Physics, 2002, 179, 578-592.	3.8	14
90	An efficient numerical method for the two-fluid Stokes equations with a moving immersed boundary. Computer Methods in Applied Mechanics and Engineering, 2008, 197, 2147-2155.	6.6	14

#	Article	IF	CITATIONS
91	Modeling a semiâ€flexible filament in cellular Stokes flow using regularized Stokeslets. International Journal for Numerical Methods in Biomedical Engineering, 2011, 27, 2021-2034.	2.1	14
92	Recent advances in renal hypoxia: insights from bench experiments and computer simulations. American Journal of Physiology - Renal Physiology, 2016, 311, F162-F165.	2.7	14
93	Cardiovascular benefits of <scp>SGLT</scp> 2 inhibition in diabetes and chronic kidney diseases. Acta Physiologica, 2018, 222, e13050.	3.8	14
94	A model of mitochondrial O ₂ consumption and ATP generation in rat proximal tubule cells. American Journal of Physiology - Renal Physiology, 2020, 318, F248-F259.	2.7	14
95	Modeling the circadian regulation of the immune system: Sexually dimorphic effects of shift work. PLoS Computational Biology, 2021, 17, e1008514.	3.2	14
96	A Semi-Lagrangian Semi-Implicit Numerical Method for Models of the Urine Concentrating Mechanism. SIAM Journal of Scientific Computing, 2002, 23, 1526-1548.	2.8	13
97	An efficient numerical method for distributed-loop models of the urine concentrating mechanism. Mathematical Biosciences, 2003, 181, 111-132.	1.9	13
98	Role of UTB Urea Transporters in the Urine Concentrating Mechanism of the Rat Kidney. Bulletin of Mathematical Biology, 2007, 69, 887-929.	1.9	13
99	Nitric oxide and superoxide transport in a cross section of the rat outer medulla. II. Reciprocal interactions and tubulovascular cross talk. American Journal of Physiology - Renal Physiology, 2010, 299, F634-F647.	2.7	13
100	Modelling female physiology from head to Toe: Impact of sex hormones, menstrual cycle, and pregnancy. Journal of Theoretical Biology, 2022, 540, 111074.	1.7	13
101	Haemodynamic frailty – A risk factor for acute kidney injury in the elderly. Ageing Research Reviews, 2021, 70, 101408.	10.9	12
102	Mathematical modeling of kidney transport. Wiley Interdisciplinary Reviews: Systems Biology and Medicine, 2013, 5, 557-573.	6.6	11
103	Use of Angiotensin-Converting Enzyme Inhibitors and Angiotensin II Receptor Blockers During the COVID-19 Pandemic: A Modeling Analysis. PLoS Computational Biology, 2020, 16, e1008235.	3.2	11
104	Sex-Specific Computational Models of Kidney Function in Patients With Diabetes. Frontiers in Physiology, 2022, 13, 741121.	2.8	11
105	A numerical method for renal models that represent tubules with abrupt changes in membrane properties. Journal of Mathematical Biology, 2002, 45, 549-567.	1.9	10
106	A velocity decomposition approach for moving interfaces in viscous fluids. Journal of Computational Physics, 2009, 228, 3358-3367.	3.8	10
107	Signal transduction in a compliant short loop of Henle. International Journal for Numerical Methods in Biomedical Engineering, 2012, 28, 369-383.	2.1	10
108	Impacts of active urea secretion into pars recta on urine concentration and urea excretion rate. Physiological Reports, 2013, 1, .	1.7	10

#	Article	IF	CITATIONS
109	An Immersed Interface Method for Axisymmetric Electrohydrodynamic Simulations in Stokes flow. Communications in Computational Physics, 2015, 18, 429-449.	1.7	10
110	Bifurcation study of blood flow control in the kidney. Mathematical Biosciences, 2015, 263, 169-179.	1.9	10
111	Intraarterial Microdosing: A Novel Drug Development Approach, Proof-of-Concept PET Study in Rats. Journal of Nuclear Medicine, 2015, 56, 1793-1799.	5.0	10
112	His and her mathematical models of physiological systems. Mathematical Biosciences, 2021, 338, 108642.	1.9	10
113	Expanding the scope of quantitative FRAP analysis. Journal of Theoretical Biology, 2010, 262, 295-305.	1.7	9
114	Tubular fluid flow and distal NaCl delivery mediated by tubuloglomerular feedback in the rat kidney. Journal of Mathematical Biology, 2014, 68, 1023-1049.	1.9	9
115	Recent advances in renal hemodynamics: insights from bench experiments and computer simulations. American Journal of Physiology - Renal Physiology, 2015, 308, F951-F955.	2.7	9
116	Impact of sex and pathophysiology on optimal drug choice in hypertensive rats: Quantitative insights for precision medicine. IScience, 2021, 24, 102341.	4.1	9
117	On the efficiency of spectral deferred correction methods for time-dependent partial differential equations. Applied Numerical Mathematics, 2009, 59, 1629-1643.	2.1	8
118	Feedback-mediated dynamics in a model of coupled nephrons with compliant thick ascending limbs. Mathematical Biosciences, 2011, 230, 115-127.	1.9	8
119	Signal transduction in a compliant thick ascending limb. American Journal of Physiology - Renal Physiology, 2012, 302, F1188-F1202.	2.7	8
120	Impact of nitric oxide-mediated vasodilation on outer medullary NaCl transport and oxygenation. American Journal of Physiology - Renal Physiology, 2012, 303, F907-F917.	2.7	8
121	Intraâ€Target Microdosing (ITM): A Novel Drug Development Approach Aimed at Enabling Safer and Earlier Translation of Biological Insights Into Human Testing. Clinical and Translational Science, 2017, 10, 337-350.	3.1	8
122	Cell Volume Regulation in the Proximal Tubule of Rat Kidney. Bulletin of Mathematical Biology, 2017, 79, 2512-2533.	1.9	8
123	An Optimization Algorithm for a Distributed-Loop Model of an Avian Urine Concentrating Mechanism. Bulletin of Mathematical Biology, 2006, 68, 1625-1660.	1.9	7
124	Maximum Urine Concentrating Capability inÂaÂMathematical Model of the Inner Medulla ofÂtheÂRatÂKidney. Bulletin of Mathematical Biology, 2010, 72, 314-339.	1.9	7
125	Hyperfiltration and inner stripe hypertrophy may explain findings by Gamble and coworkers. American Journal of Physiology - Renal Physiology, 2010, 298, F962-F972.	2.7	7
126	Optimizing SGLT inhibitor treatment for diabetes with chronic kidney diseases. Biological Cybernetics, 2019, 113, 139-148.	1.3	7

#	Article	IF	CITATIONS
127	Determining risk factors for triple whammy acute kidney injury. Mathematical Biosciences, 2022, 347, 108809.	1.9	7
128	Fluid dilution and efficiency of Na ⁺ transport in a mathematical model of a thick ascending limb cell. American Journal of Physiology - Renal Physiology, 2013, 304, F634-F652.	2.7	6
129	Predicted effects of nitric oxide and superoxide on the vasoactivity of the afferent arteriole. American Journal of Physiology - Renal Physiology, 2015, 309, F708-F719.	2.7	6
130	Modeling the effects of positive and negative feedback in kidney blood flow control. Mathematical Biosciences, 2016, 276, 8-18.	1.9	6
131	A new microscope for the kidney: mathematics. American Journal of Physiology - Renal Physiology, 2017, 312, F671-F672.	2.7	6
132	Pathophysiological mechanisms underlying a rat model of triple whammy acute kidney injury. Laboratory Investigation, 2020, 100, 1455-1464.	3.7	6
133	The furosemide stress test and computational modeling identify renal damage sites associated with predisposition to acute kidney injury in rats. Translational Research, 2021, 231, 76-91.	5.0	6
134	A METHODOLOGY FOR TRACKING SOLUTE DISTRIBUTION IN A MATHEMATICAL MODEL OF THE KIDNEY. Journal of Biological Systems, 2005, 13, 399-419.	1.4	5
135	New numerical methods for Burgers' equation based on semi-Lagrangian and modified equation approaches. Applied Numerical Mathematics, 2010, 60, 645-657.	2.1	5
136	Oxygen transport in a cross section of the rat inner medulla: Impact of heterogeneous distribution of nephrons and vessels. Mathematical Biosciences, 2014, 258, 68-76.	1.9	5
137	An Exact Solution for Stokes Flow in a Channel with Arbitrarily Large Wall Permeability. SIAM Journal on Applied Mathematics, 2015, 75, 2246-2267.	1.8	5
138	A Semi-Lagrangian Collocation Method for the Shallow Water Equations on the Sphere. SIAM Journal of Scientific Computing, 2003, 24, 1433-1449.	2.8	4
139	Role of structural organization in the urine concentrating mechanism of an avian kidney. Mathematical Biosciences, 2005, 197, 211-230.	1.9	4
140	Tubuloglomerular Feedback Signal Transduction inÂaÂShortÂLoop of Henle. Bulletin of Mathematical Biology, 2010, 72, 34-62.	1.9	4
141	Fluid extraction across pumping and permeable walls in the viscous limit. Physics of Fluids, 2016, 28, 041902.	4.0	4
142	Conduction of feedback-mediated signal in a computational model of coupled nephrons. Mathematical Medicine and Biology, 2016, 33, 87-106.	1.2	4
143	Quadratic spline methods for the shallow water equations on the sphere: Collocation. Mathematics and Computers in Simulation, 2006, 71, 187-205.	4.4	3
144	Renal tubular solute transport and oxygen consumption. Current Opinion in Nephrology and Hypertension, 2018, 27, 384-389.	2.0	3

#	Article	lF	CITATIONS
145	Multiscale models of kidney function and diseases. Current Opinion in Biomedical Engineering, 2019, 11, 1-8.	3.4	3
146	Quadratic spline methods for the shallow water equations on the sphere: Galerkin. Mathematics and Computers in Simulation, 2006, 71, 175-186.	4.4	2
147	Transfer Function Analysis of Dynamic Blood Flow Control in the Rat Kidney. Bulletin of Mathematical Biology, 2016, 78, 923-960.	1.9	2
148	Sweet success? SGLT2 inhibitors and diabetes. American Journal of Physiology - Renal Physiology, 2018, 314, F1034-F1035.	2.7	2
149	Solute and water transport along an inner medullary collecting duct undergoing peristaltic contractions. American Journal of Physiology - Renal Physiology, 2019, 317, F735-F742.	2.7	2
150	Recent advances in renal epithelial transport. American Journal of Physiology - Renal Physiology, 2019, 316, F274-F276.	2.7	2
151	Tubuloglomerular feedback signal transduction in a model of a compliant thick ascending limb. FASEB Journal, 2008, 22, 761.3.	0.5	2
152	Waveform distortion in TGFâ€mediated limitâ€cycle oscillations: Effects of TAL flow. FASEB Journal, 2009, 23, .	0.5	2
153	Sexâ€specific Computational Models for Blood Pressure Regulation in the Rat. FASEB Journal, 2019, 33, 758.6.	0.5	2
154	Accurate computation of Stokes flow driven by an open immersed interface. Journal of Computational Physics, 2012, 231, 5195-5215.	3.8	1
155	Interface methods for biological and biomedical problems. International Journal for Numerical Methods in Biomedical Engineering, 2012, 28, 289-290.	2.1	1
156	Modeling Blood Flow Control in the Kidney. The IMA Volumes in Mathematics and Its Applications, 2015, , 55-73.	0.5	1
157	Theoretical assessment of the Ca2+ oscillations in the afferent arteriole smooth muscle cell of the rat kidney. International Journal of Biomathematics, 2018, 11, 1850043.	2.9	1
158	A Multicellular Vascular Model of the Renal Myogenic Response. Processes, 2018, 6, 89.	2.8	1
159	Tubular Fluid Oscillations Mediated by Tubuloglomerular Feedback in a Short Loop of Henle. FASEB Journal, 2012, 26, 690.1.	0.5	1
160	Impact of nitric oxideâ€mediated vasodilation on outer medullary NaCl transport and oxygenation. FASEB Journal, 2012, 26, 1100.6.	0.5	1
161	Mathematical Modeling of Urea Transport in the Kidney. Sub-Cellular Biochemistry, 2014, 73, 31-43.	2.4	1
162	An optimization study of a mathematical model of the urine concentrating mechanism of the rat kidney. Mathematical Biosciences, 2010, 223, 66-78.	1.9	0

#	Article	IF	CITATIONS
163	Introduction to Mathematical Modeling of Blood Flow Control in the Kidney. Association for Women in Mathematics Series, 2017, , 63-73.	0.4	Ο
164	Computing viscous flow along a 2D open channel using the immersed interface method. Engineering Reports, 2021, 3, e12334.	1.7	0
165	Dynamics in coupled nephrons may contribute to irregular flow oscillations in spontaneously hypertensive rats. FASEB Journal, 2006, 20, A759.	0.5	0
166	Estimation of Collecting Duct Parameters for Maximum Urine Concentrating Capability in a Mathematical Model of the Rat Inner Medulla. FASEB Journal, 2006, 20, A1224.	0.5	0
167	Maximum Urine Concentrating Capability for Transport Parameters and Urine Flow within Prescribed Ranges. FASEB Journal, 2007, 21, A905.	0.5	Ο
168	A mathematical model of the afferent arteriolar smooth muscle cell. FASEB Journal, 2010, 24, 1059.27.	0.5	0
169	Efficiency of sodium transport in a model of the Thick Ascending Limb (TAL). FASEB Journal, 2011, 25, .	0.5	Ο
170	Dynamical Properties of the Thick Ascending Limb (TAL): A Modeling Study. FASEB Journal, 2011, 25, 665.8.	0.5	0
171	Role of UTB Urea Transporters in the Urine Concentrating Mechanism of the Rat Kidney. FASEB Journal, 2011, 25, 840.1.	0.5	Ο
172	Interactions between Tubuloglomerular Feedback and the Myogenic Mechanism of the Afferent Arteriole. FASEB Journal, 2012, 26, 690.2.	0.5	0
173	Role of interstitial nodal spaces in the urine concentrating mechanism of the rat kidney. FASEB Journal, 2012, 26, 1100.8.	0.5	Ο
174	Urine Concentrating Mechanism: Impact of Vascular and Tubular Architecture and a Proposed Descending Limb Ureaâ€Na Cotransporter. FASEB Journal, 2012, 26, 1100.11.	0.5	0
175	Nephrovascular interactions in a mathematical model of rat renal autoregulation. FASEB Journal, 2013, 27, 1110.5.	0.5	Ο
176	Modeling the effects of medullary blood flow regulation on pressure natriuresis. FASEB Journal, 2013, 27, 1111.2.	0.5	0
177	Tubuloglomerular Feedback. Lecture Notes on Mathematical Modelling in the Life Sciences, 2014, , 85-106.	0.4	0
178	Nitric Oxide and Superoxide Significantly Affect Medullary Oxygenation and Urinary Output. FASEB Journal, 2015, 29, 963.1.	0.5	0
179	Urinary PO2 as a biomarker for medullary hypoxia. FASEB Journal, 2015, 29, 963.6.	0.5	0
180	Implications of Increased Renal Venous Pressure for Renal Hemodynamic and Reabsorptive Function Studied by a Mathematical Model of the Kidney. FASEB Journal, 2015, 29, 808.19.	0.5	0

#	ARTICLE	IF	CITATIONS
181	SGLT2 Inhibition Is Predicted to Increase NaCl Delivery to the Medullary Thick Ascending Limb But Not to Significantly Elevate Its Oxygen Consumption. FASEB Journal, 2015, 29, 959.3.	0.5	0
182	Internephron Coupling Increases the Efficiency of Dynamic Autoregulation. FASEB Journal, 2016, 30, 739.6.	0.5	0
183	Modeling Blood Flow and Oxygenation in a Diabetic Rat Kidney. Association for Women in Mathematics Series, 2017, , 101-113.	0.4	0
184	Tracking the Distribution of a Solute Bolus in the Rat Kidney. Association for Women in Mathematics Series, 2017, , 115-136.	0.4	0
185	His and Her Computational Models of Longâ€ŧerm Blood Pressure Regulation. FASEB Journal, 2018, 32, 714.5.	0.5	0
186	Determining Risk Factors for Triple Whammy AKI using Computational Models of Long―Term Blood Pressure Regulation. FASEB Journal, 2019, 33, 758.5.	0.5	0
187	Functional Implications of Sexual Dimorphism of Transporter Patterns along the Rat Nephron. FASEB Journal, 2019, 33, 864.1.	0.5	0
188	Impact of shifting epithelial Na + transport on renal medullary oxygen tension: Modeling and analysis. FASEB Journal, 2019, 33, 748.1.	0.5	0
189	Title is missing!. , 2020, 16, e1008235.		Ο
190	Title is missing!. , 2020, 16, e1008235.		0
191	Title is missing!. , 2020, 16, e1008235.		0
192	Title is missing!. , 2020, 16, e1008235.		0
193	Title is missing!. , 2020, 16, e1008235.		0
194	Title is missing!. , 2020, 16, e1008235.		0
195	Intrarenal Reninâ€Angiotensin System and its Role in Angiotensin IIâ€Induced Hypertension: Insights from Computational Modelling. FASEB Journal, 2022, 36, .	0.5	Ο
196	Renal adaptations in gestational hypertension preserves K ⁺ while minimizing Na ⁺ retention. FASEB Journal, 2022, 36, .	0.5	0
197	A predictive model for estimating protection against CKD and CVD with SGLT2 inhibition in patients with diabetes. FASEB Journal, 2022, 36, .	0.5	Ο